



Identification of small scale *in situ* soft-sediment deformation structures using ground penetrating radar, an example from Permian submarine slope deposits of the Karoo Basin, South Africa

CARLOS M. M. OLIVEIRA^{(1,2)*}, JOHN HAKES⁽²⁾ & DAVID HODGSON⁽²⁾

⁽¹⁾Petrobras S.A. – Exploration and Production. Av República do Chile, 65, Rio de Janeiro RJ, Brazil), ⁽²⁾University of Liverpool, Department of Earth and Ocean Sciences. 4 Brownlow Street, Liverpool U.K.

Copyright 2009, SBGf - Sociedade Brasileira de Geofísica

This paper was prepared for presentation during the 11th International Congress of the Brazilian Geophysical Society held in Salvador, Brazil, August 24-28, 2009.

Contents of this paper were reviewed by the Technical Committee of the 11th International Congress of the Brazilian Geophysical Society and do not necessarily represent any position of the SBGf, its officers or members. Electronic reproduction or storage of any part of this paper for commercial purposes without the written consent of the Brazilian Geophysical Society is prohibited.

Abstract

Intervals of soft-sediment deformation features including vertical fluid escape and load structures are common and well exposed in Permian lower slope deposits of the Tanqua Depocentre, Karoo Basin. The structures comprise mainly elongated flames, and load structures associated with ruptured sandstones and structureless siltstones, observed over a range of scales. Analysis of around 180 flame structures up to 2 m high, indicated they are oriented SW-NE, parallel to the deepwater palaeoslope in lateral splay deposits between two major slope channel complexes. Ground penetrating radar profiles confirm the overall NE orientation of the flame structures and provide a basis for recognition of potential larger-scale examples of flames in seismic reflection datasets.

Keywords GPR, Karoo Basin, *in situ* deformation, soft-sediment deformation structures, flame structures.

Introduction

Soft-sediment deformation structures is a collective term used to describe a variety of features that occur at a wide range of scales and form via mechanisms that promote the ductile deformation of sediments. *In situ* soft-sediment deformation occurs without significant down slope movement (less than a few metres of dislocation) and generates smaller structures, typically below seismic resolution. A large range of structures can be generated by *in situ* deformation as a function of the direction of particle dislocation; if vertical, horizontal or a combination.

The study area is located at Waterfall, within the Tanqua depocentre, Karoo Basin, South Africa, and focuses on a 30 m thick succession of Permian submarine slope deposits of Skoorsteenberg Formation Unit 5, exposed over a 4 km² area. The Waterfall section is a shallow gully formed by the confluence of several ephemeral streams; the local topography provides good 3D control on the exposed deformation features. The 30 m thick interval is characterized by three facies groups; (1) interbedded sandstone and siltstone, (2) bedded sandstone and (3) deformed sandstone and siltstone. A typical logged section shows the vertical arrangement of facies groups

1, 2 and 3. Deformation is characterized by vertically-oriented and commonly hourglass-shaped, siltstone dominant, flame structures, that dissect folded fine-grained sandstone beds. Seven sedimentary logs were collected and measurements of geometrical parameters and orientation were obtained from 180 flame structures from seven intervals. Measurements of geometrical attributes and orientations were analysed and indicated that the studied flame structures are elongated and oriented SW-NE, reaching up 2 m high.

The aim of this paper is to show the use of GPR to characterize the shape and orientation of products of *in situ* soft-sediment deformation processes, represented mainly by intervals of flame structures in the submarine slope deposits of the Karoo Basin.

Methodology and dataset

The use of the GPR method for the study of sedimentary rocks is largely focused on architectural and stratigraphic characterization (Neal, 2004, and references therein). Fractures, faults and folds generate reflections not related to the primary sedimentary bedding that can generate major electromagnetic discontinuities responsible for the deterioration of the GPR image quality; this can lead to misinterpretation when such events are not properly identified. Faults and fractures are the most common vertical structures identified in GPR profiles (Green *et al.*, 2003; Rossetti, 2003; Theune *et al.*, 2006), in scales varying from a few metres (Reiss *et al.*, 2003) to hundreds of metres (Bakker & Van der Meer, 2003).

a. Planning and acquisition

The first step was to establish the geological objective and the general configuration of the survey. A 600 m² survey was acquired on a flat surface of sandstone (free of soil cover), targeting flame structures 2-5 m below the surface and extrapolated from the outcrop face, with the objective of imaging the flame shapes and verifying their orientations. Inlines were oriented N30E, spaced 1 m from each other, and positioned to obtain the best possible coverage of the outcrop, while the cross-lines were positioned 5 m from each other and at 90° from the in-lines. This configuration was oblique to the general orientation of flames (WSW-ENE) from the adjacent outcrops and arranged in order to contemplate the range of scale of the studied structures and, at the same time, to attend questions of logistic and time. The occurrence of one flame in a vertical face contiguous with the survey helped in the determination of the acquisition parameters.

Identification of soft-sediment structures using GPR

Two acquisition techniques were used in Waterfall: (i) the common offset or reflection sound and (ii) the common mid point (CMP). The first was used to map the subsurface discontinuities in the whole survey. The second was used to measure the velocity of the sedimentary package.

The acquisition parameters (Table 1) were chosen to ensure penetration of 4 m, coupled with the best possible vertical resolution. Among the acquisition parameters, the nominal antenna frequency, the vertical stack and step size were analysed. The vertical resolution is given by $\lambda/2$ to $\lambda/4$ where λ is the wavelength. If $\lambda = v/f$, and $v=0.12$ m/ns, obtained from the CMP survey, then the vertical resolution for a frequency of 100 MHz will vary between 0.6 m and 0.3 m, while for 200 MHz it will vary between 0.3 m and 0.15 m. Both are in the range of the bed thicknesses at Waterfall. The step size was chosen to be tight (0.1 m) in order to improve the lateral resolution. The two antennae (transmitter and receiver) were oriented orthogonal to the line direction with separation varying between 0.5 m (200 MHz) and 1.0m (100 MHz) in order to avoid signal saturation in the top portion of the trace, following test and quality analysis in the field. The separation of 1 m for 100 MHz satisfied the empirical relationship that the separation must be 20% of the target depth (Jol & Bristow, 2003) while the separation of 0.5 m for the 200 MHz survey was at the limit for the base of one deformed interval.

b. Processing

Although simpler compared to the processing involved of seismic reflection data, the processing of GPR data follows the same steps used for seismic data. Basically, the objective is to recover the signal for deeper reflectors where amplitude is diminished by attenuation and to increase the signal:noise ratio. The basic workflow for the processing is presented in Table 1 and was defined after a series of tests that involved the inclusion of other steps like deconvolution and FK filtering in some special cases.

The same workflow, with some changes in the parameters, was used to process the two different sets of lines (100 MHz and 200 MHz). In general, the quality of the lines was poor but better in the set acquired with 100 MHz frequency (Figure 1). Among the factors that affected the quality of the GPR in Waterfall, the most important were: (i) rock homogeneity (siltstones and fine sandstones), (ii) the verticality of the flame structures and (iii) the problems with coupling the equipment with the rock surface. The 200 MHz lines were not able to image the depth of the flame structures probably because of the ringing in the upper reflectors and wrong definition of the acquisition parameters (for example small separation). The steps and parameters used for processing are briefly described below:

- Data preparation: due to the flat surface it was not necessary to undertake a static correction for topographic effects; the dead traces were removed and the first arrival was moved to time zero (time-zero drift correction);
- Signal-saturation correction (dewowing): a dewowing filter (5 ns window) was used to remove the “wow”

induced by signal saturation due to the airwave, ground-wave and near-surface wave;

- Application of gain: this was used to amplify the weak signal at the level of the objective, due to progressive attenuation with increase in travel time. The AGC was applied with window length=25ns and scaling factor=1). This amplified the weak, deeper signal, but required equalisation of amplitude of all signals and noise.
- Application of filters: normally one bandpass filter ($f = \{30,70,270,310\}$) was used, based on analysis of the frequency spectrum, to eliminate very low and very high amplitudes, normally associated with noise. In lines WFA104 and WFA105, a localized (spike shape) high amplitude value was identified, with the peak frequency around 144MHz. This was interpreted as a product of the acquisition equipment, which caused a deterioration of the signal/noise ratio. It was removed using a notch filter ($f = \{136,142,147,151\}$).
- Migration: Kirchhoff's migration (velocity = 0.12 ns) was applied in order to remove the effects of diffractions and distortions.

Interpretation

The interpretation of the GPR lines focused on two aspects: (i) to identify radar facies and to correlate them with Waterfall lithofacies, and (ii) to confirm the orientation of the flame structures. The structures are identified in the GPR profiles by their vertical shape, by the lateral changing in the signal amplitude and truncations, and by the bent reflectors. In line Wf101, a clearly imaged vertical feature, characterized by low amplitude and discontinuous internal horizons, appears at the SW limit of the line and is interpreted as the expression of a flame structure (Figure 1). A flame structure of similar size and shape at the same stratigraphic interval can be observed at outcrop, 10 m from the GPR line. The laterally continuous high amplitude folded horizon positioned at 40 ns is interpreted as the expression of the ruptured sandstones. Just above and truncating the high amplitude folded horizon is a continuous low amplitude horizon that is interpreted as the capping homogeneous siltstone linked to the flames. The radar facies of the vertical structure (flame) and the truncating horizon are quite similar. At 20ns, a very high amplitude horizon just above the highest vertical feature and truncating the underlying horizons can be directly correlated to the main level of top scours and infill in the parent outcrop.

Based on the identified features, five horizons were interpreted (Figure 1a), affected to different degrees by the soft-sediment deformation structures: (1) base of “red” reflector, related to the topographic low above the flames; (2) and (3) top and base of the “blue” interval, at the top section of the interval between the main level of flames and the base of the “red” reflector, probably associated with a ruptured bed; (4) “violet” reflector, associated with the base of the structureless siltstone; and (5) “orange” section, representing the main interval of flames. The interpretation was based on stacked (i.e. not-migrated) and migrated GPR sections. The presence of diffractions and distortions in non-migrated sections was related to the soft-sediment structures and used to help the interpretation.

Figure 2 summarizes the distribution and 2D dimensions (along inlines and crosslines) of the radar features interpreted as products of soft-sediment deformation. This interpretation was based on the stratigraphic level of the occurrence compared to the position in the face of the adjacent outcrop and dimensions of the local exposed structures. This single map permits the observation of the effect of the flame structure on the five distinct horizons: where just one colour is present it means that the structure is affecting just one level; superposition of colours means that the structure is disrupting distinct beds. After the interpretation and plot of the distinct structures, a WSW-ENE trend and a secondary N-S trend of the "ellipse bodies" were mapped. The main trend coincides with the orientation of the flame structures in the nearby outcrops. It is important to emphasize that better constraint for the flame orientation would be obtained if the controlling lines (crosslines) were closer.

Conclusion

The GPR results indicate that at sub-seismic scales, the main structural and lithological variations related to the deformational features correspond to a radar-facies change. The study shows that elongate flame structures (i) can be identified both vertically and horizontally by the GPR method, (ii) can extend horizontally further (at least few metres) than is observed in outcrop and (iii) can be organized forming parallel trends of structures. Additionally, this study indicates that GPR provides a high resolution link to the likely expression of geometrically similar but larger features that could occur in high resolution seismic reflection datasets. The use of GPR in the study of small scale soft-sediment deformation is rarely cited in the literature (Liberty *et al.*, 2003). Therefore, the Waterfall dataset represents a relatively rare and novel applicability of GPR.

Acknowledgements

The first author thanks Petrobras for the financial support for this research that was part of his PhD project. Also, would like to thank Steve Flint from the University of Liverpool for the supervision and guidance during the research project, DeVille Wickens from the University of

Stellenbosch for field support and Amilson Rodrigues from Petrobras for the support in the data processing

References

- Bakker, M.A.J. & Van der Meer, J.J.M.** (2003) Structure of a Pleistocene push moraine revealed by GPR: the eastern Veluwe Ridge, The Netherlands. *In: Bristow, C.S. & Jol, H.M. (eds) Ground Penetrating Radar in Sediments*. Geological Society, London, Special Publication, **211**, 143-151.
- Green, A., Gross, R., Holliger, K., Horstmeyer, H. & Baldwin, J.** (2003) Results of 3-D georadar surveying and trenching the san Andreas fault near its northern landward limit. *Tectonophysics*, **368**, 7-23.
- Jol, H.M. & Bristow, C.S.** (2003) GPR in sediments: advice on data collection, basic processing and interpretation, a good practice guide. *In: Bristow, C.S. & Jol, H.M. (eds) Ground Penetrating Radar in Sediments*. Geological Society, London, Special Publication, **211**, 9-27.
- Liberty, L.M., Hemphill-Haley, M.A. & Madin, I.P.** (2003) The Portland Hills Fault: uncovering a hidden fault in Portland, Oregon using high-resolution geophysical methods. *Tectonophysics*, **368**, 89-103.
- Neal, A.** (2004) Ground-penetrating radar and its use in sedimentology: principles, problems and progress. *Earth-Sciences Reviews*, **66**, 261-330.
- Reiss, S., Reicherter, K.R. & Reuther, C-D.** (2003) Visualization and characterization of active normal faults and associated sediments by high-resolution GPR. *In: Bristow, C.S. & Jol, H.M. (eds) Ground Penetrating Radar in Sediments*. Geological Society, London, Special Publication, **211**, 247-255.
- Rosseti, D.F.** (2003) Delineating shallow Neogene deformation structures in northeastern Pará State using Ground Penetrating Radar. *Anais da Academia Brasileira de Ciências*, **75**, 235-248.
- Theune, U., Rokosh, D., Sacchi, M.D. & Schmitt D.R.** (2006) Mapping fractures with GPR: A case study from Turtle Mountain. *Geophysics*, **71**, B139-B150.

Identification of soft-sediment structures using GPR

Acquisition Parameters		Processing workflow
Nominal antenna frequency	100MHz / 200MHz	Remove dead traces
Pulse Voltage	400V	Time cut
Recording length	512ns	Dewowing
Sample interval	0.8ns	AGC
Vertical stack	32	(Notchfilter)
Separation	1.0m (100MHz) 0.5m (200MHz)	Bandpass filter
Step size	0.1m	(Deconvolution)
		Migration

Table 1: Ground penetrating radar (GPR) survey acquisition and processing parameters.

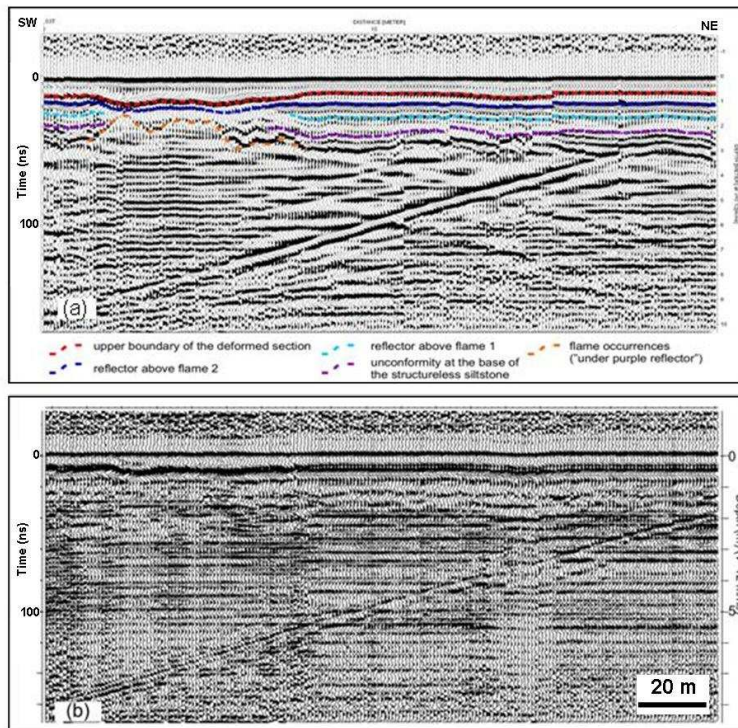


Figure 1: Comparison of line Wf101 acquired with the frequencies of 100 MHz (a) and 200 MHz (b). Interpretation and mapping of 5 horizons were made in the 100MHz set of GPR lines (a).

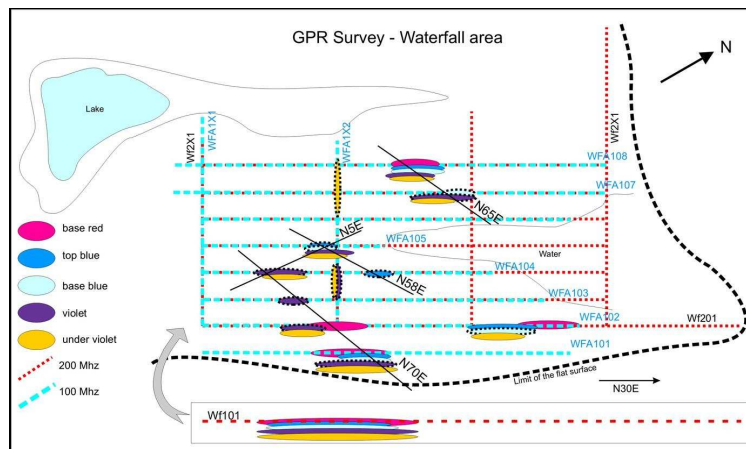


Figure 2: GPR survey for 200 and 100MHz and the distribution of seismic features as the response of soft-sediment deformation considering distinct horizons. Line Wf101 was shot in the same position as line WFA102.